

Cite this: DOI: 10.1039/c4cp06116k

www.rsc.org/pccp

Supplementary
Information

On the importance of shear dissipative forces in coarse-grained dynamics of molecular liquids

Sergei Izvekov^{*a} and Betsy M. Rice^a

Received 30th December 2014, Accepted 11th March 2015

DOI: 10.1039/c4cp06116k

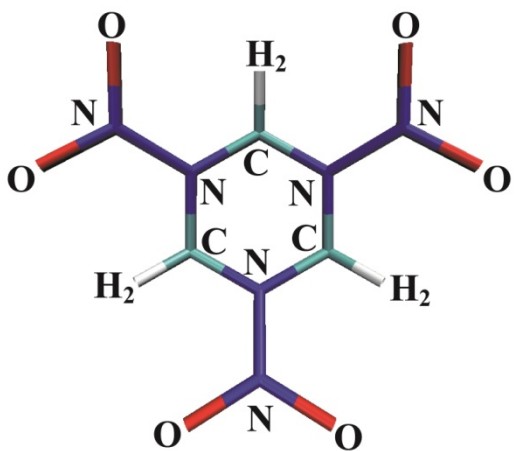


Fig. S1 Molecular structure of RDX.

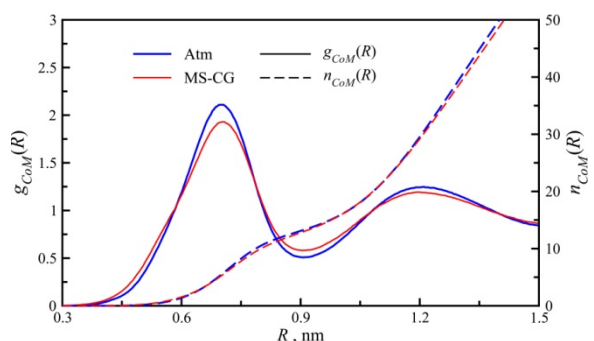


Fig. S2 Comparison of the molecular CoM RDF, $g_{CoM}(R)$, from the reference atomistic simulation (blue solid) and the CG RDF (red solid) obtained with the MS-CG model. The dashed lines display the corresponding running integration numbers, $n_{CoM}(R)$.

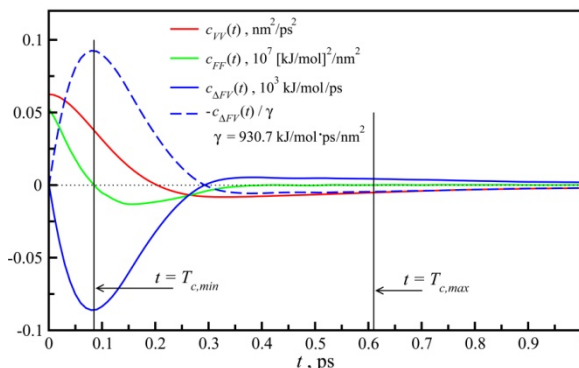


Fig. S3 Molecular CoM correlation functions $c_{VV}(t)$, $c_{FF}(t)$, and $c_{\Delta FV}(t)$ from atomistic simulation. The vertical solid lines mark the atomistic characteristic time scales $T_{c,min}$, $T_{c,max}$. The dashed line displays $-c_{\Delta FV}(t)$, which is rescaled with a friction $\gamma = 930.7$ kJ/mol·ps/nm² (1 kJ/mol·ps/nm² = 1.660539 × 10⁻¹⁵ kg/s) to highlight the agreement of $c_{\Delta FV}(t)$ (blue solid) and $c_{VV}(t)$ (red) on Markovian time scales, $t > T_{c,max}$.

1. Gaussian smoothing of frictions $\gamma^{\parallel}(R)$, $\gamma^{\perp}(R)$, $\gamma^{eff}(R)$

The correlations $c_{\Delta FV}^{\alpha}$, $c_{VV}^{\alpha\beta}$ and frictions $\gamma^{\parallel}(R)$, $\gamma^{\perp}(R)$, $\gamma^{eff}(R)$ were obtained in the form of histograms, i.e., $\{c_{VV}^{\alpha\beta}(t, R_l), l = 1, \dots, N_{bin}\}$ on an equally-spaced mesh with a bin size of $\Delta R = R_{cut}^f / N_{bin} = 0.0025$ nm. For the production DPD simulations, the frictions were smoothed out as

$$\gamma(R) \approx \Delta R \sum_{l=1}^{N_{bin}} \gamma(R_l) G(R - R_l) \quad (S1)$$

by applying a Gaussian filter¹

$$G(R) = \frac{1}{\sqrt{2\pi}\sigma} e^{-\frac{R^2}{2\sigma^2}} H\left(1 - \frac{|R|}{\sigma'}\right), \quad (S2)$$

where the $H(t)$ is the Heaviside function and σ is the bandwidth parameter which controls the smoothness of the filtered profile. For a chosen σ (we selected $\sigma = 6\Delta R$), the σ' is selected to have $G(\sigma') = \varepsilon$, where the tolerance $\varepsilon = 10^{-3}$.

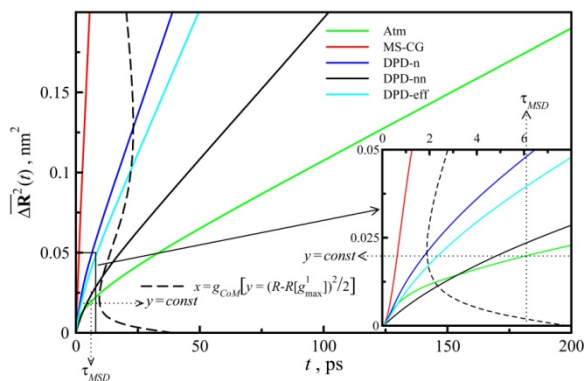


Fig. S4 Comparison of MSD, $\overline{\Delta R^2}$, from atomistic (green), MS-CG (red), DPD-n (blue), DPD-nn (black), and DPD-eff (cyan) simulations of RDX melt. Insets enlarge the countered regions as indicated by arrows. The black dashed line shows the curve $x = g_{CoM}(y)$, where $y = (R - R[g_{max}^1])^2 / 2$. A solution of eqn (23), τ_{MSD} , for atomistic system can be determined graphically as time at which the $\overline{\Delta R^2}(t)$ curve (green) crosses a horizontal line $y = const$, which passes through minimum of $g_{CoM}(y)$, as illustrated in the plot by dotted lines.

2. Velocity autocorrelation functions (VACF), $c_{VV}(t)$, and the vibrational density of states (VDOS) spectra, $\tilde{c}_{VV}(\lambda)$, for liquid and crystal RDX

Comparison of the liquid VACF and VDOS from atomistic, MS-CG, and MS-CG/DPD models is shown in Fig. S5a and Fig. S6a. The atomistic CG VDOS is the vibrational spectrum of the molecular translational motion and has a single-band structure with the peak positioned at 25 cm^{-1} . The MS-CG VDOS has a two-band structure, in which the major low-frequency peak is located at 10 cm^{-1} . Similar to liquid NM,¹ the comparison of the MS-CG and atomistic CG spectra suggests that the major translational band in the atomistic system develops due to conservative forces. The second narrow shoulder-like band in the MS-CG VDOS reflects oscillating behaviour in the corresponding $c_{VV}(t)$ that is suppressed in the atomistic and DPD models due to friction. The DPD-n model predicts more accurately the position and amplitude of the peak in the atomistic CG VDOS and thus better captures the initial caged dynamics in which the molecule repeatedly attempts to leave the first coordination shell. The location of the band in the DPD-n VDOS is in between the locations of the two major bands in the MS-CG

VDOS. The DPD-nn and DPD-eff models, in which the friction is greater, overdamp the MS-CG VDOS causing the band to shift toward low frequencies. An overall similarity between the atomistic CG and DPD-n vibrational spectra further suggests that the interactions governing the distinct short-range molecular liquid structure of the RDX have major contributions from both the shear dissipative and conservative forces.

The above conclusion is supported by a comparison of the $c_{VV}(t)$ for the crystal phase at $T = 300 \text{ K}$ as shown in Fig. S5b. Since the liquid MS-CG potential is not transferable to crystalline

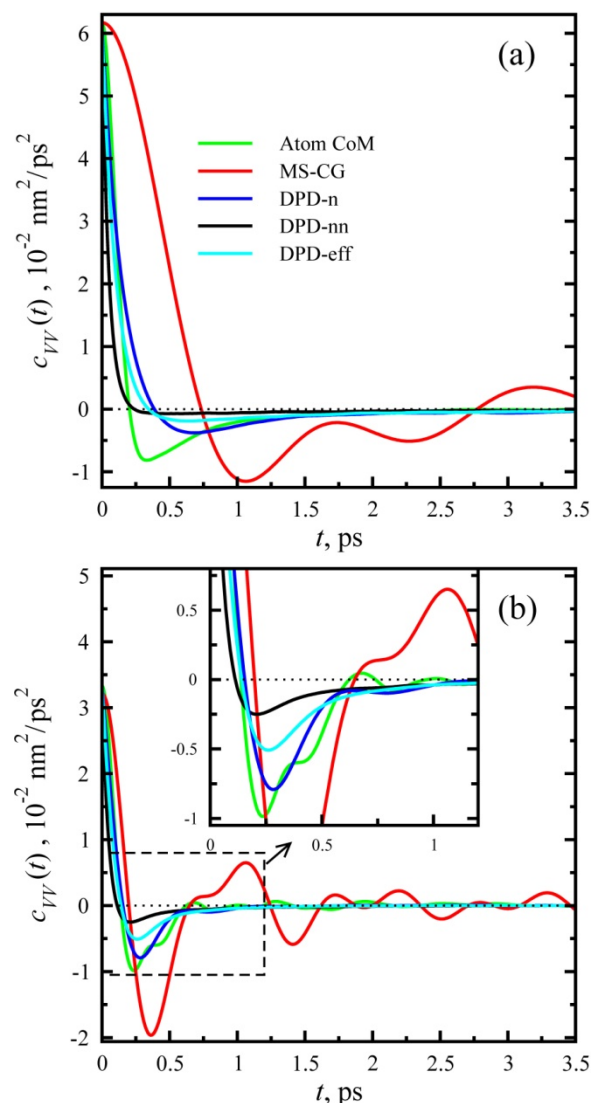


Fig. S5 Comparison of the CoM $c_{VV}(t)$ from atomistic (green), MS-CG (red), DPD-n (blue), DPD-nn (black), and DPD-eff (cyan) simulations of the RDX melt [Panel (a)] and bulk crystal [Panel (b)] systems. The inset in panel (b) is an enlargement of the region enclosed by the dashed line.

systems, we used the density-dependent MS-CG model of RDX developed in Ref.² to treat the crystal. Fig. S5b demonstrates good agreement in the shapes of the $c_{VV}(t)$ compared to the liquid. In particular, the strength of the negative autocorrelations is reproduced well, and the agreement progressively improves for

the model with less dissipation, i.e. with faster D_{diff} , with the DPD-n model showing the best result. The crystal spectra $\tilde{c}_{VV}(\lambda)$ are compared in Fig. S6b. Although the shapes of the $c_{VV}(t)$ agree between the crystal and the liquid CG VDOS, the crystal CG VDOS exhibits multiple bands, with the leading band of the liquid VDOS is split into the three peaks located between 35 and 50 cm^{-1} and a shoulder-shaped feature at 100 cm^{-1} . The conservative MS-CG model reproduces the leading three bands, however the model amplifies them into narrow peaks while shifting the bands to lower frequencies. The atomistic VDOS up to 25 cm^{-1} is captured well by all three DPD models. The DPD-n

importance of shear dissipation to capture such dynamics accurately. For RDX, it points to the dominance of the γ^{\perp} across different phases, and not limited to the liquid phase. This result was not expected, since it is known that in coarse-grained elastic networks the Markovian approximation is violated due to strong acoustic phonon-mediated memory effects.³⁻⁴ Although in weakly interacting molecular crystals the long-ranged dynamics carried out by acoustical phonons is damped, it is still may impact adversely the performance of the MS-CG/DPD models, especially at low temperatures. Such was not the case for our system.

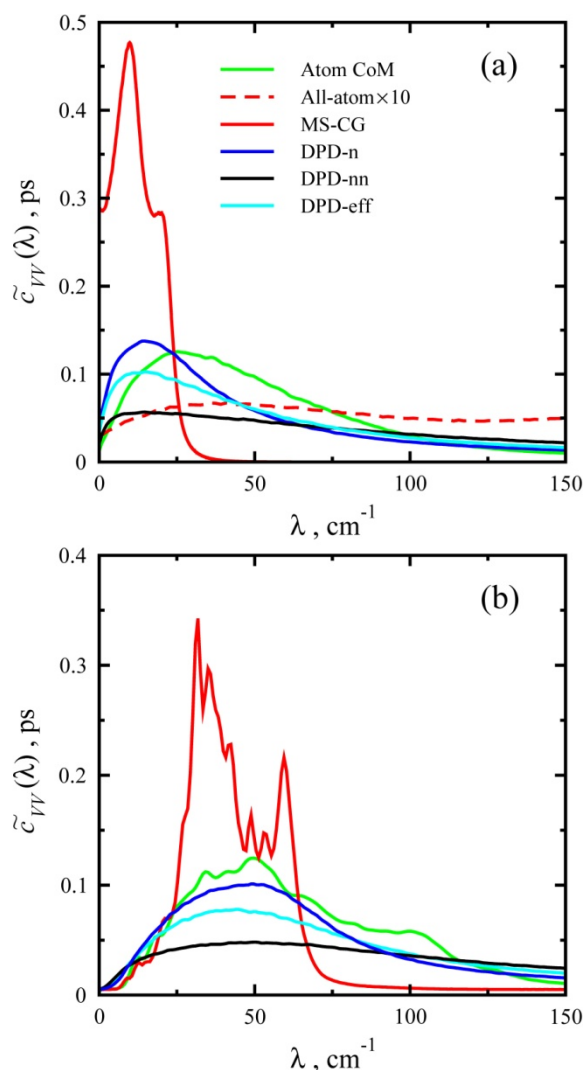


Fig. S6 Power spectra $\tilde{c}_{VV}(\lambda)$ [eqn (20)] of $c_{VV}(t)$ from Fig. S5.

In panel (a), the dashed line shows the atomistic $\tilde{c}_{VV}(\lambda)$ for the melt, and is scaled up by a factor of ten.

model yields a nearly perfectly shaped VDOS which resembles the atomistic VDOS with the secondary band structure smoothed out. The agreement is somewhat surprising considering the fact that the conservative interaction used for the crystal system is different from that used in the liquid. However, the crystal dynamics is essentially caged dynamics and hence the fact that it is well represented by the DPD-n model further suggests an

Notes and references

^a Weapons and Materials Research Directorate, U.S. Army Research Laboratory, Aberdeen Proving Ground, Maryland 21005, USA; E-mail sergiy.izvekov.civ@mail.mil

1. S. Izvekov and B. M. Rice, *J. Chem. Phys.*, 2014, **140**, 104104.
2. S. Izvekov, P. W. Chung and B. M. Rice, *J. Chem. Phys.*, 2011, **135**, 044112.
3. D. Cubero and S. N. Yaliraki, *J. Chem. Phys.*, 2005, **122**, 034108.
4. D. Kauzlaric, J. T. Meier, P. Espanol, S. Succi, A. Greiner and J. G. Korvink, *J. Chem. Phys.*, 2011, **134**, 064106.